High-resolution kinetics of herbivore-induced plant volatile transfer reveal tightly clocked responses in neighboring plants

Jamie M. Waterman, Lei Wang, Tristan M. Cofer and Matthias Erb

Institute of Plant Sciences, University of Bern, Bern, Switzerland

Corresponding authors:

jamie.waterman@unibe.ch (JMW);

matthias.erb@unibe.ch (ME)

Abstract

Volatiles emitted by herbivore-attacked plants (senders) can enhance defenses in neighboring plants (receivers), with important consequences for community dynamics. However, the temporal dynamics of this phenomenon remain poorly studied. Using a custom-built, high-throughput proton transfer reaction time-of-flight mass spectrometry (PTR-ToF-MS) system, we explored temporal patterns of volatile transfer and responses between herbivore-attacked and undamaged maize plants. We found that continuous exposure to natural blends of herbivore-induced volatiles results in distinct temporal response patterns in neighboring plants, characterized by an induced terpene burst at the onset of the second day of exposure. This delayed burst is not explained by terpene accumulation during the night, but coincides with delayed jasmonate accumulation in receiver plants. The delayed burst occurs independent of day:night light transitions and cannot be fully explained by sender volatile dynamics. Instead, it is the result of a clocked stress memory from volatile exposure during the first day and secondary exposure to bioactive volatiles on the second day. Our study reveals that prolonged exposure to natural blends of stress-induced volatiles results in a response that integrates priming and direct induction into a distinct and predictable temporal response pattern, with potentially important consequences for plant-herbivore dynamics and tritrophic interactions. This work also contributes to answering the long-standing question of whether stress volatiles predominantly induce or prime plant defenses in neighboring plants.

Introduction

Plants rely on chemical cues to identify and mount appropriate responses to herbivores [1,2]. Among these cues are herbivore-induced plant volatiles (HIPVs) [3,4]. When perceived by

undamaged plants, HIPVs can enhance plant defenses, and thus increase plant resistance to future herbivory [5–9]. HIPVs can directly induce plant defenses [7,8,10,11]. HIPVs can also prime plant defenses. In this case, HIPV-exposed plants respond more strongly and/or more rapidly to a secondary stimulus such as herbivore attack [5,7,8,12].

Plant responses to environmental cues depend on temporal dynamics. For example, artificial damage that mimics spatiotemporal patterns of chewing herbivores induces a similar response to actual herbivore attack [13]. The emission of HIPVs also follows discrete temporal dynamics [5,14], which, again, is likely to influence defense responses in receiver plants. Green leaf volatiles (GLVs), including (*Z*)-3-hexenyl acetate, (*Z*)-3 hexenal and (*Z*)-3-hexen-1-ol are catabolic products of the lipoxygenase/hydroperoxide lyase pathway and are emitted within minutes following damage [15,16]. Indole and terpenes are emitted within hours of herbivore attack [2,5]. Indole can mediate interactions between plants as well as between plants and other organisms [17–19]. Terpenes are a very diverse group of volatile (> 80,000 known structures) that are also important as both direct and indirect plant defenses [6,20–22]. Indole and terpenes take longer to produce in comparison to GLVs and are less transiently emitted [2,5,15]. In maize, GLVs have been implicated in direct induction [8,10], and both GLVs and indole are known to prime defenses, and are thus considered as 'bioactive' in information transfer between plants [5,7].

Although it is clear that plants can either be primed or directly induced following HIPV exposure, if and how these two phenomena integrate in the context of a natural HIPV exposure sequence is unclear. Studies have yet to monitor induction and priming dynamics in real time and during continuous exposure to HIPVs. It is possible that, through time, continuous HIPV exposure may result in a self-enforced positive feedback loop, whereby priming enhances induction and induction serves as a priming event for subsequent induction. Further, temporal trends might be complicated by dynamic environmental conditions, such as

light fluctuations; over a 24 hr period, plants can experience both full sun and darkness. In darkness, the emission of many volatiles, especially those released via stomata, is severely hindered [23–26].

In order to understand the kinetics of information transfer between plants and the importance of dynamic temporal emission patterns, we monitored the emission kinetics of terpenes as a marker of defense activation in maize plants that were exposed to HIPVs. We leveraged a highly temporally-resolved volatile multiplexing system that allowed us to track continuous volatile emissions in sender and receiver plants for the first time in real time. We further measured terpene pools, stress hormones and defense gene expression in receiver plants, and determined the impact of day:night light transitions in the observed defense induction kinetics. Finally, we measured defenses upon sequences of short-term HIPV and GLV exposure to unravel the relative importance of direct induction and priming. Together, our experiments reveal how the natural kinetics of herbivore attack result in a tightly clocked defense response in neighboring plants via volatile information transfer.

Results

Delayed burst in induced volatile emissions in plants exposed to volatiles of an herbivore-attacked neighbor

When maize plants are exposed to volatiles from herbivore-attacked neighbors, they start to release terpenes [7,11]. To understand the temporal dynamics of this phenomenon, we conducted a detailed time-course analysis of terpene release by receiver plants exposed to volatiles from sender plants under attack by *Spodoptera exigua* caterpillars (Fig 1). Within 2

hr, we detected a small induction of sesquiterpenes, monoterpenes, 4,8-dimethylnona-1,3,7-triene (DMNT) and 4,8,12-trimethyltrideca-1,3,7,11-tetraene (TMTT) in undamaged receiver plants. This response disappeared at night. Interestingly, as soon as the night was over, we observed a strong burst of terpene release from receiver plants, which was 2-5 times higher than the release the day before (Fig 1). Thus, exposure to volatiles from an herbivore-attacked plant triggers a delayed burst in terpene emission in neighboring plants.

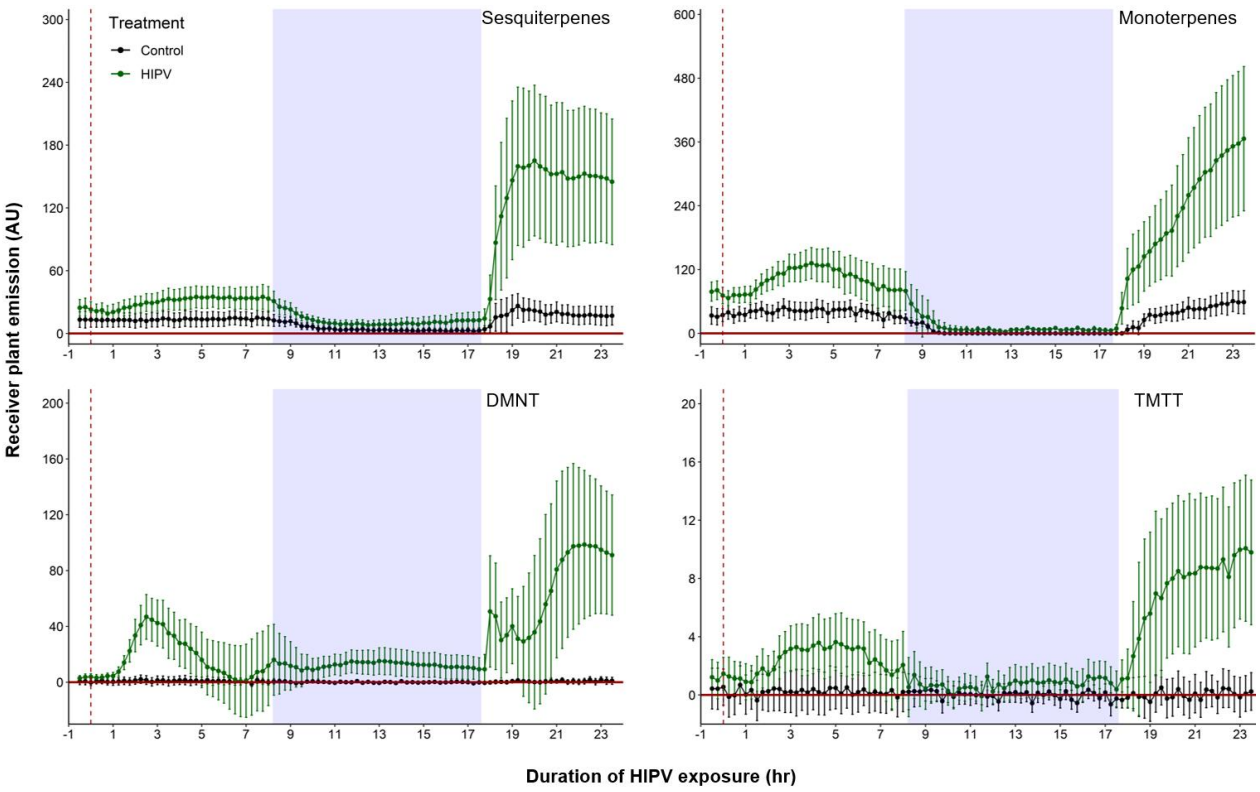

Figure 1. Delayed burst in induced volatile emissions in plants exposed to volatiles of a herbivore-attacked neighbor. Emission kinetics of herbivore-induced plant volatile (HIPV)-induced terpenes in undamaged receiver plants are shown. Dark green points represent mean emission of herbivore-damaged sender plants connected to undamaged receiver plants, with the emissions from damaged sender plants only subtracted. Black points represent the same but with undamaged sender plants. Blue rectangle represents the dark phase. Abbreviations. DMNT, 4,8-dimethylnona-1,3,7-triene; TMTT, 4,8,12-trimethyltrideca-1,3,7,11-tetraene. Error bars = SE. *n* = 8-10.

The delayed burst in terpene emission is not explained by overaccumulation during the night

Why do receiver plants show a delayed burst in volatile-induced terpenoid release? During the night, plants close their stomata to limit water loss [27], which may also impair terpene release, thus leading to an accumulation of terpenes in the leaves and a burst once stomata open again [23,28]. To determine if terpenes (over)accumulate in maize leaves of HIPV-exposed plants during the night, we measured internal foliar pools of the major sesquiterpenes, β-caryophyllene, β-farnesene, and α-bergamotene, as well as the homoterpene TMTT over time. Internal pools of β-caryophyllene, β-farnesene and TMTT started increasing after 3 hours, but only became significant after 8 hr of exposure to HIPVs (Fig 2A, 2B and 2D, Table 1). For all three, accumulation remained higher during the night (16.75 hr) as well as the following day. α-bergamotene only began accumulating in leaves on the second day (Fig 2C, Table 1). Thus, internal sesquiterpene pools remain comparable between night and day, suggesting that even when volatiles are emitted in large amounts on day two, internal pools do not deplete below nighttime levels. To get insight into terpene biosynthesis we measured the expression of terpene synthases. In maize, farnesene pyrophosphate synthase 3 (FPPS3), terpene synthase 2 and 10 (TPS2 and TPS10) as well as dimethylnonatriene/trimethyltetradecatetraene synthase (CYP92C5) are rate limiting for terpene production [29–31]. All genes were induced by HIPV exposure during daytime, but not during the nighttime. FPPS3 was slightly induced after 3 hr and significantly induced after 8 hr HIPV exposure (Fig 2E, Table 1). TPS2 was slightly induced 3, 8 and 22 hr after the onset of HIPV exposure (Fig 2F, Table 1). TPS10 was significantly induced after 3 and 22 hr of HIPV exposure (Fig 2G, Table 1). CYP92C5 was only significantly induced after 3 hr of HIPV exposure (Fig 2H, Table 1). The patterns of volatile terpene biosynthesis do not

support a scenario where the terpene burst on the second day is due to continued biosynthesis but lack of emission during the night.

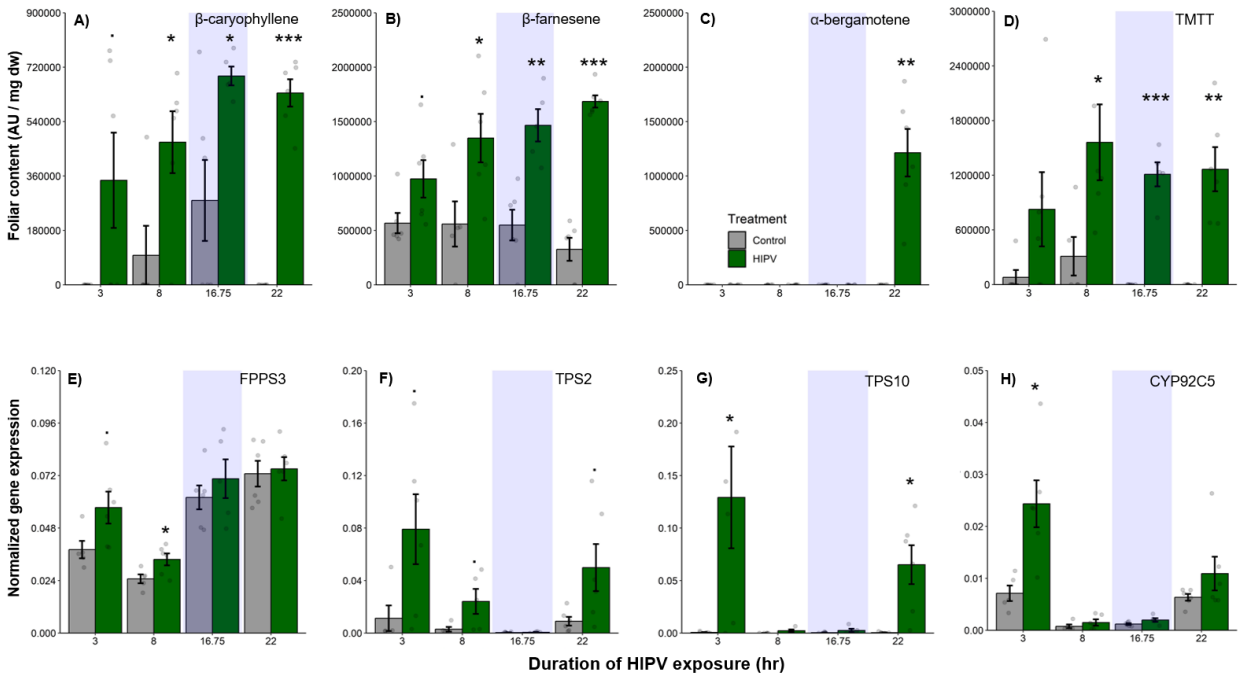

Figure 2. The delayed burst in terpene emission is not explained by terpene overaccumulation during the night. Accumulation of terpenes and induction of terpene biosynthesis genes in receiver plants was measured over time. A-D) Internal foliar pools of terpenes in receiver plants. E-H) Expression of terpene biosynthesis genes in receiver plants. Dark green bars represent receiver plants exposed to herbivore-induced plant volatiles (HIPVs) and light grey bars represent receiver plants exposed to control plant volatiles. Blue rectangle represents the dark phase. Abbreviations: TMTT, 4,8,12-trimethyltrideca-1,3,7,11-tetraene; FPPS3, Farnesyl pyrophosphate synthase 3; TPS2, Terpene synthase 2; TPS10, Terpene synthase 10; CYP92C5, Dimethylnonatriene/trimethyltetradecatetraene synthase. . = $p < 0.1$, * = $p < 0.05$, ** = $p < 0.01$, *** = $p < 0.001$ as determined by a Welch's two-sample *t*-test. Bars = mean ± SE. n = 4-6.

The delayed burst in terpenoid emission is associated with clocked jasmonate production

Volatile release in maize is regulated by jasmonates [32,33]. To understand whether the delayed terpene burst is associated with jasmonate signaling, we measured the levels of 12-oxo-phytodienoic acid (OPDA), jasmonic acid (JA) and jasmonic acid-isoleucine (JA-Ile), as

well as the expression of oxo-phytodienoate reductase 7 (OPR7), which is critical for JA biosynthesis [34]. We found a significant induction of OPDA, JA-Ile production and OPR7 expression at the beginning of the second day, 22 hr after the onset of volatile exposure (Fig 3, Table 1). Thus, jasmonate production is temporally aligned with the delayed terpene burst at the onset of the second day.

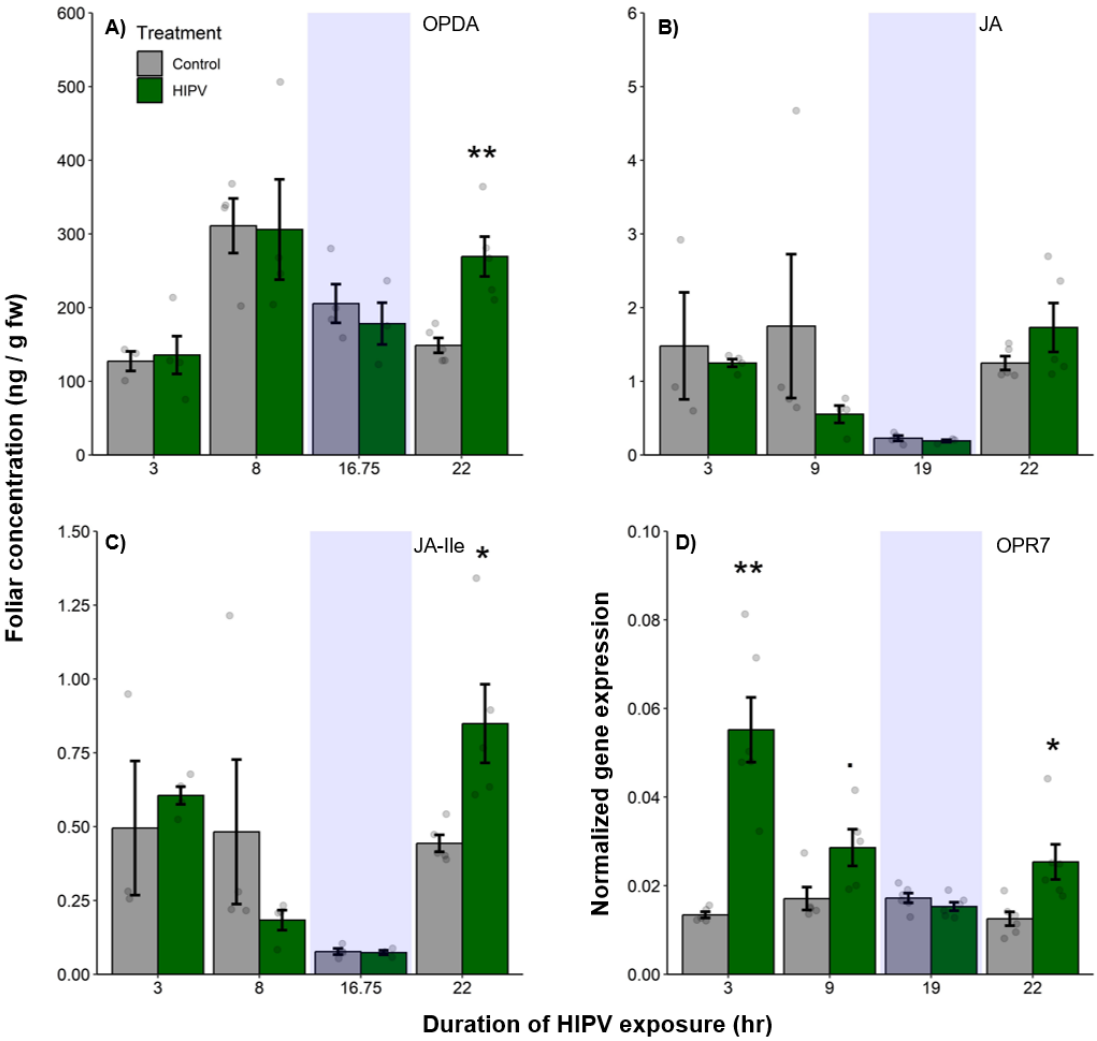

Figure 3. The delayed burst in terpene emission is associated with clocked jasmonate production. Foliar jasmonate concentrations (A-C) and jasmonate biosynthesis (OPR7; D) in receiver plants over time are shown. Dark green bars represent receiver plants exposed to herbivore-induced plant volatiles (HIPVs) and light grey bars represent receiver plants exposed to control plant volatiles. Blue rectangle represents the dark phase. Abbreviations. OPDA = 12-oxophytodienoic acid, JA = jasmonic acid, JA-Ile = jasmonic acid-isoleucine, OPR7 = oxo-phytodienoate reductase 7. . = $p < 0.1$, * = $p < 0.05$, ** = $p < 0.01$, *** = $p < 0.001$ as determined by a Welch's two-sample *t*-test. Bars = mean ± SE. n = 3-6.

Table 1. Welch's two-sample *t*-test results for foliar terpene pools, biosynthesis genes and phytohormone levels. Bold values: $p < 0.05$, underlined values: $p < 0.1$. Abbreviations: β-car, β-caryophyllene; β-farn, β-farnesene; α-berg, α-bergamotene; TMTT, 4,8,12-trimethyltrideca-1,3,7,11-tetraene; FPPS3, Farnesyl pyrophosphate synthase 3; TPS2, Terpene synthase 2; TPS10, Terpene synthase 10; CYP92C5, Dimethylnonatriene/trimethyltetradecatetraene synthase; OPDA = 12-oxophytodienoic acid; JA = jasmonic acid; JA-Ile = jasmonic acid-isoleucine; OPR7 = oxo-phytodienoate reductase 7.

	Time											
Response	3 hr			8 hr			16.75 hr			22 hr		
	t	*p*	df	*t*	*p*	df	*t*	*p*	df	*t*	*p*	df
β-car	-2.20	<u>0.08</u>	5	-2.65	**0.03**	9	-3.00	**0.03**	6	-14.05	**<0.001**	5
β-farn	-2.08	<u>0.07</u>	8	-2.60	**0.03**	9	-4.47	**0.002**	9	-11.38	**<0.001**	8
α-berg	-	-	-	-	-	-	-	-	-	-5.56	**0.003**	5
TMTT	-1.80	0.13	5	-2.68	**0.03**	7	-9.18	**<0.001**	4	-5.23	**0.003**	5
FPPS3	-2.31	<u>0.05</u>	8	-2.62	**0.03**	9	-0.82	0.44	7	-0.28	0.78	10
TPS2	-2.39	<u>0.05</u>	6	-2.19	<u>0.09</u>	4	-0.62	0.55	8	-2.24	<u>0.07</u>	5
TPS10	-2.65	**0.05**	5	-1.97	0.12	4	-1.34	0.25	4	-3.50	**0.02**	5
CYP92C5	-3.62	**0.01**	6	-1.11	0.30	8	-1.94	0.11	5	-1.38	0.22	5
OPDA	-0.26	0.80	4	0.07	0.95	5	0.65	0.55	4	-4.18	**0.008**	5
JA	0.32	0.78	2	1.22	0.31	3	0.91	0.41	4	-1.40	0.22	5
JA-Ile	-0.48	0.68	2	1.21	0.31	3	0.24	0.82	5	-2.98	**0.04**	4
OPR7	-5.70	**0.002**	5	-2.36	<u>0.05</u>	7	1.32	0.22	10	-3.01	**0.02**	7

The delayed volatile burst is conserved under continuous light

To test whether the delayed burst in terpene volatiles is linked to light:dark transitions, we exposed maize plants to HIPVs under continuous light. Similar to exposure during a normal light regime, the largest burst of terpene emission occurred *ca.* 15-18 hr after the onset of volatile exposure (Fig 4), suggesting that the temporal delay in volatile emission in receiver plants is not dependent on light fluctuations, but is otherwise clocked (Fig 4).

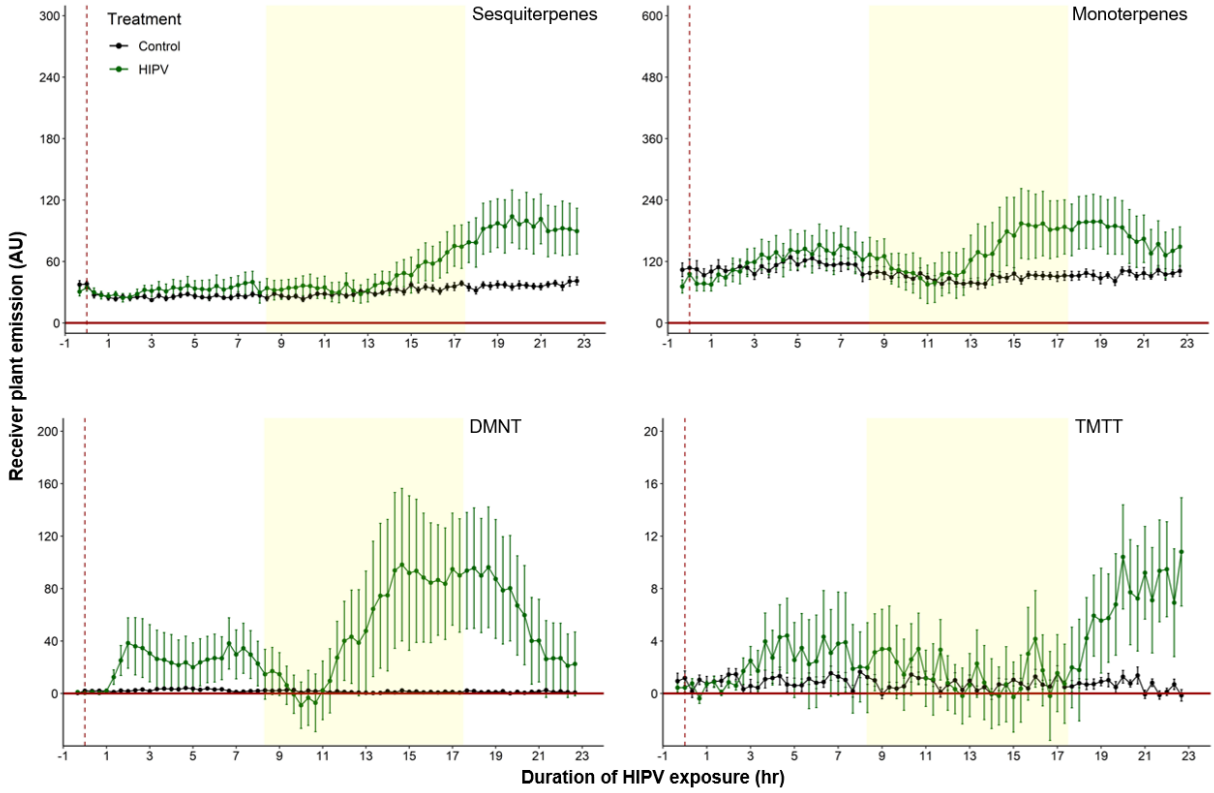

Figure 4. The delayed volatile burst is conserved under continuous light. Emission kinetics of herbivore-induced plant volatiles (HIPV)-induced terpenes in undamaged receiver plants under continuous light are shown. Dark green points represent the mean emission of herbivore damaged sender plants connected to undamaged receiver plants with the emissions from damaged sender plants only subtracted. Black points represent the same but with undamaged sender and receiver plants. Yellow rectangle represents when the lights would typically be turned off. Abbreviations: DMNT, 4,8-dimethylnona-1,3,7-triene; TMTT, 4,8,12-trimethyltrideca-1,3,7,11- tetraene. Error bars = SE. *n* = 8-10.

The delayed volatile burst cannot be fully explained by the emission kinetics of bioactive herbivory-induced volatiles

A simple explanation for the delayed volatile burst may be that the bioactive volatiles are more strongly emitted from sender plants at the onset of day two, thus triggering a stronger volatile response in the receiver plants at this time. To test this hypothesis, we analyzed

volatile emission kinetics of *S. exigua*-infested plants over time. We focused our analysis on GLVs and indole, which are known to induce and/or prime volatile release in neighboring maize plants [7,8,10,11]. Terpenes are not known prime or induce volatile release in maize, and were thus not included in the sender plant analysis [11]. We analyzed GLV and indole emission data of the sender plants from the experiments depicted in Fig 1 and Fig 4 (Fig 5), and then correlated their emission with the induction of terpenes in receiver plants (Fig. 6). We found strong positive correlations between hexenal, hexenyl acetate, hexen-1-ol and indole emissions in sender plants and terpene responses in receiver plants when plants had a dark period (Fig 6). Interestingly, this was not the case under continuous light, where the magnitude of the emission of bioactive volatiles was not directly correlated to the magnitude of terpene responses in receiver plants (Fig 6). Emissions by sender plants even showed slight negative correlations with terpene induction in receiver plants under continuous light. Thus, the emission kinetics of bioactive volatiles from sender plants cannot fully explain the delayed terpene burst.

169

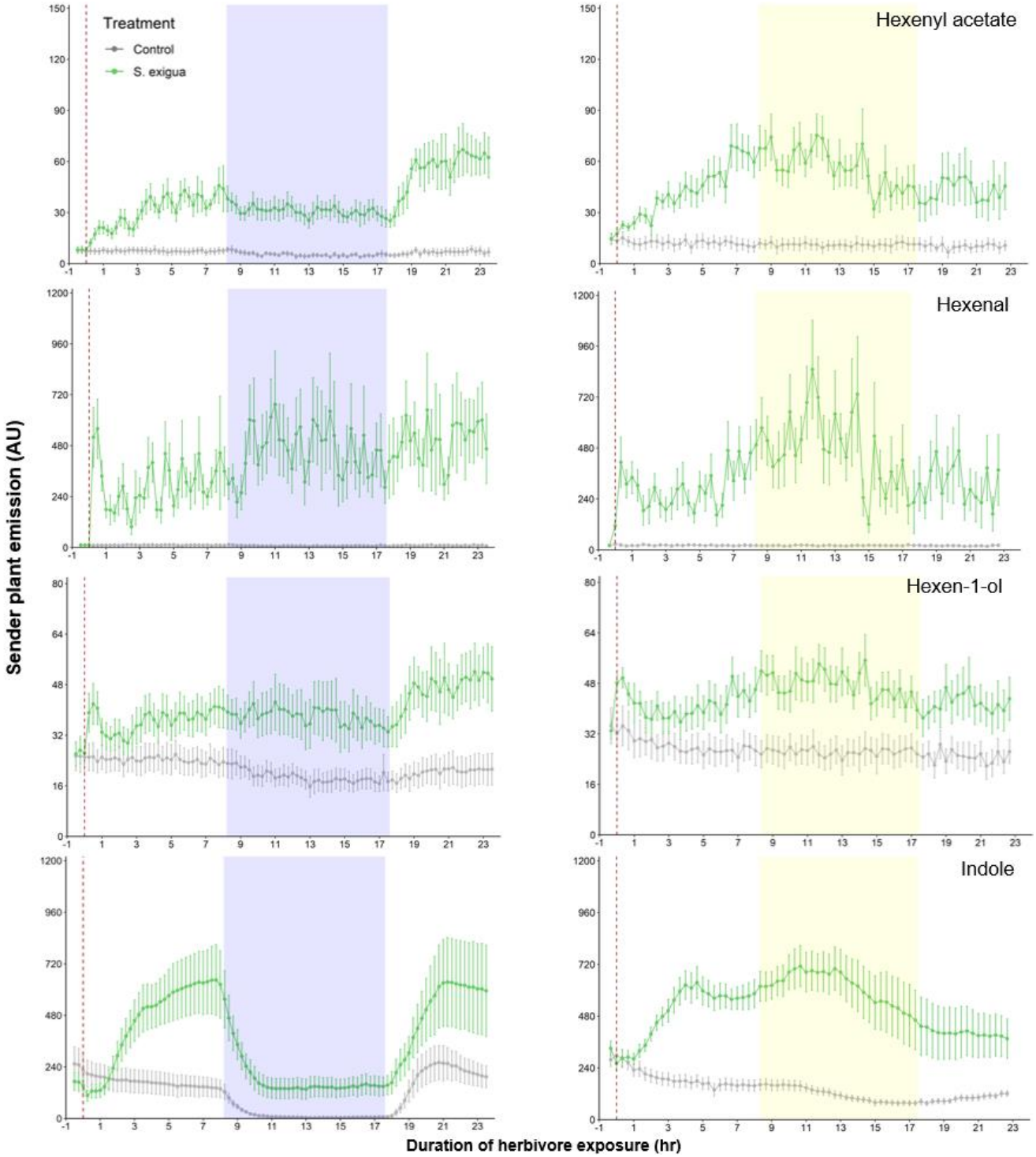

Figure 5. Green leaf volatile (GLV) and indole emissions in *Spodoptera exigua*-damaged plants. Light green points represent the mean emission of herbivore-damaged sender plants. Grey points represent the mean emission of undamaged sender plants. Blue rectangle represents the dark phase. Yellow rectangle represents when the lights would typically be turned off. Error bars = SE. *n* = 8-10.

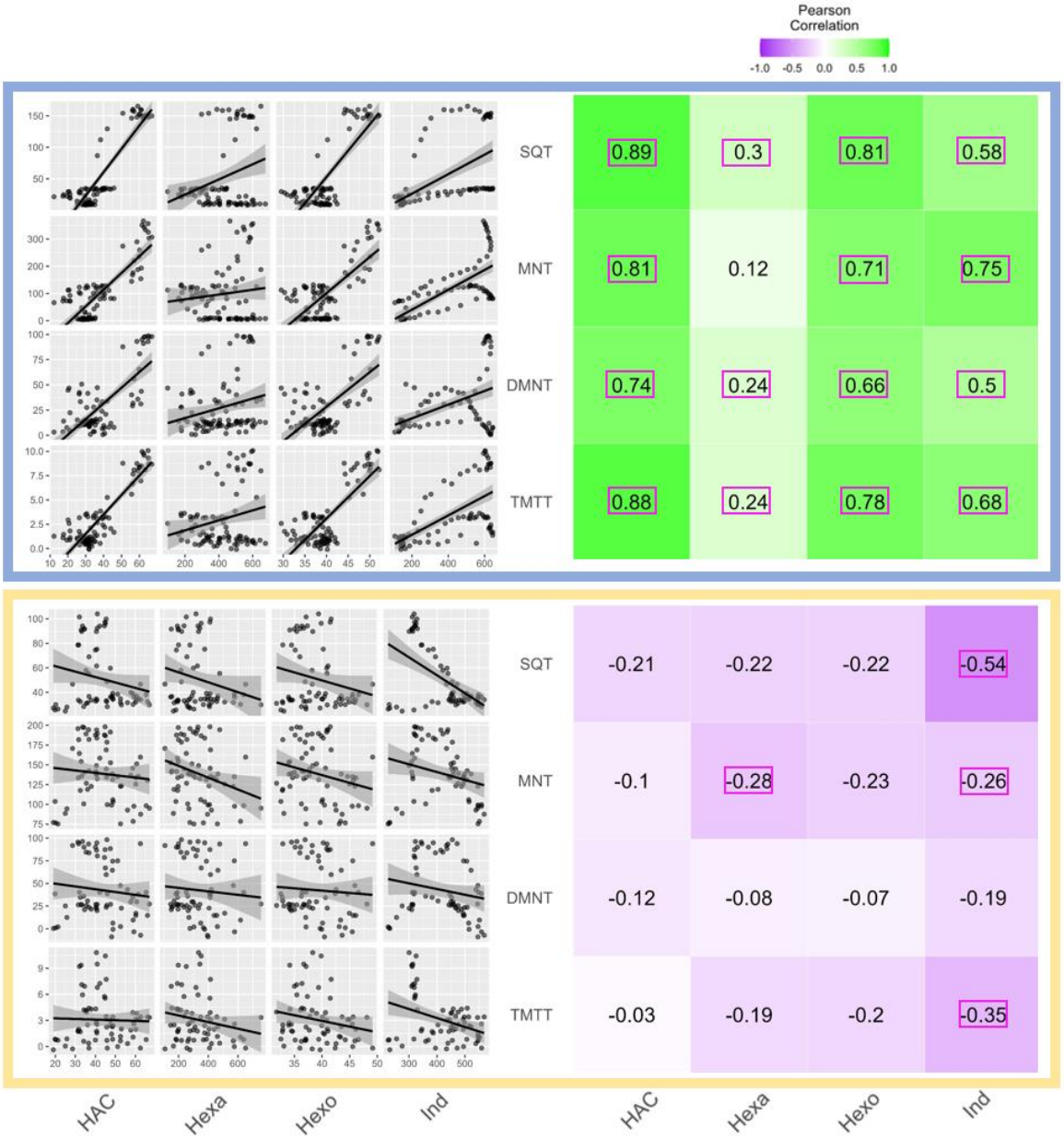

Figure 6. Receiver plant terpene emissions tightly correlate with bioactive sender plant signals under normal light conditions. The left panels depict scatter plot correlation matrices of volatile emissions from both damaged sender plants and herbivore-induced plant volatile (HIPV)-exposed receiver plants, from the first measurement following the addition of herbivores to sender plants. Upper scatter plot (in blue box) shows correlations under normal light conditions and lower scatter plot (yellow box) depicts correlations under continuous light. Each black point represents the mean value of all individuals at a given time point after herbivory began. Panels on the right hand side depict heat maps based on the value of Pearson's correlation coefficient between two given compounds. Numbers in the center of each square are Pearson's correlation coefficient. Correlation coefficients contained in a pink rectangles indicate a significant correlation ($p < 0.05$). Hexenyl acetate (HAC), Hexenal (Hexa), Hexen-1-ol (Hexo) and indole (Ind) were from sender plants, and sesquiterpenes (SQT), monoterpenes (MNT), 4,8-dimethylnona-1,3,7-triene (DMNT) and 4,8,12-trimethyltrideca-1,3,7,11-tetraene (TMTT) were from receiver plants.

The combination of direct induction and clocked priming can explain the delayed terpene burst in receiver plants

Based on the above observations, we reasoned that, under natural conditions, the strong delayed volatile burst may be due to the interaction of a volatile-induced, clocked component that primes plants for higher volatile release at the onset of the second day, and a secondary trigger in the form of bioactive volatiles released from sender plants at the onset of the second day. To test this hypothesis, we exposed receiver plants to volatiles from control plants or volatiles from herbivory-induced plants for 1.25 hr. We then disconnected the receiver plants and exposed them to clean air for 17 hr, until the beginning of the next day. Half of the plants were then exposed to (*Z*)-3-hexenyl acetate as a secondary trigger. (*Z*)-3-hexenyl acetate was selected as an inducer as it showed the strongest correlation with all measured terpenes (Fig 6). Following the short exposure to HIPVs, we detected a generally small but significant induction of sesquiterpenes, monoterpenes, DMNT and TMTT emissions in receiver plants (Fig 7, Table 2). During the night, no differences between treatments were detected any more. At the beginning of the next day, we found a slight induction in terpene emissions, most apparent for sesquiterpenes and TMTT, in plants that had been exposed to herbivory induced volatiles 18 hr prior (Fig 7, Table 2). (*Z*)-3-hexenyl acetate exposure at the beginning of the next day also induced terpene emissions. Furthermore, (*Z*)-3-hexenyl acetate induced a stronger release of all terpenes in plants that had been exposed to HIPVs the previous day. Thus, exposure to HIPVs prompts maize plants to release more terpenes the next day and also primes maize plants to respond more strongly to a secondary HIPV trigger. Together, these two phenomena result in a pronounced terpene burst.

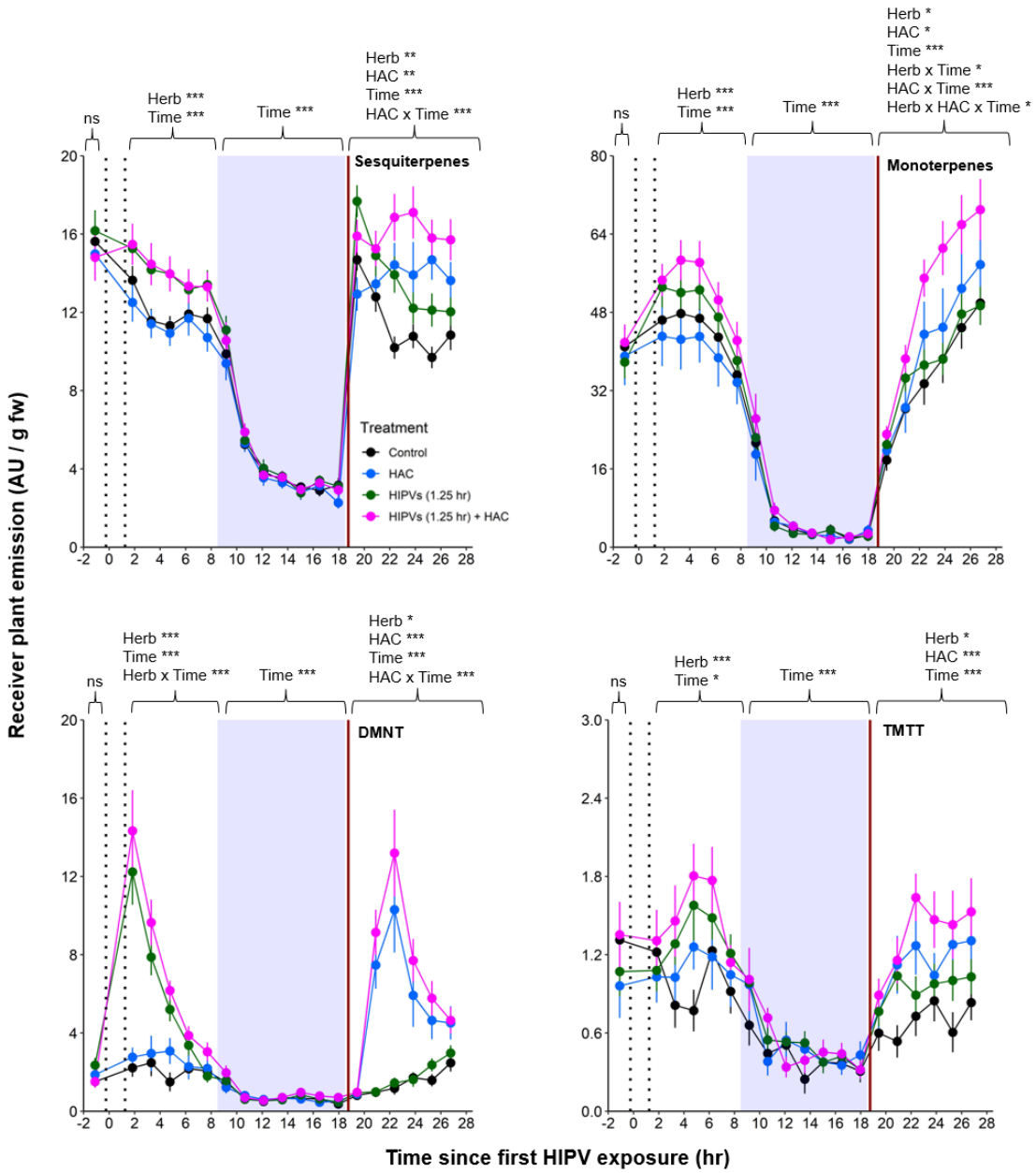

Figure 7. The combination of volatile priming and sender emission kinetics can explain the delayed terpene burst in receiver plants. Sender plants were connected to receiver plants 30 min prior to herbivore exposure on sender plants and left connected for 1.25 hr following exposure (time between perforated vertical lines). After 1.25 hr, chambers were disconnected and measurements were collected from receiver plant chambers only. The following day, after light was restored, plants were treated with (*Z*)-3-hexenyl acetate (HAC) dispensers to simulate bioactive signals (indicated by red solid vertical line). * = $p < 0.05$, ** = $p < 0.01$, *** = $p < 0.001$ as determined by aligned rank transformed nonparametric factorial repeated measures ANOVA. Abbreviations: HIPV, herbivore-induced plant volatile; DMNT, 4,8-dimethylnona-1,3,7-triene ; TMTT, 4,8,12-trimethyltrideca-1,3,7,11-tetraene. Colored points represent mean emissions standardized by fresh weight (fw). Error bars = SE. n = 12-16.

Table 2. Aligned rank transformed nonparametric factorial repeated measures ANOVA results. Bold values: $p < 0.05$ and underlined values: $p < 0.1$. Abbreviations: HAC, (Z)-3-hexenyl acetate; SQT, sesquiterpenes; MNT, monoterpenes; DMNT, 4,8-dimethylnona-1,3,7-triene ; TMTT, 4,8,12-trimethyltrideca-1,3,7,11-tetraene.

	Herb			HAC			Time			Herb x HAC			Herb x Time			Hac x Time			Herb x HAC x Time		
	F	*p*	df	*F*	*p*	df	*F*	*p*	df	*F*	*p*	df	*F*	*p*	df	*F*	*p*	df	*F*	*p*	df
SQT																					
Base	0.22	0.64	1,54	0.23	0.62	1,54	NA	NA	NA	0.05	0.82	1,54	NA	NA	NA	NA	NA	NA	NA	NA	NA
D1	13.8	**<0.001**	1,54	0.40	0.53	1,54	8.03	**<0.001**	4,216	0.30	0.59	1,54	1.85	0.12	4,216	0.10	0.98	4,216	0.23	0.92	4,216
Dark	2.15	0.15	1,54	0.17	0.69	1,54	118	**<0.001**	6,324	0.28	0.60	1,54	1.65	0.13	6,324	1.06	0.39	6,324	0.83	0.55	6,324
D2	8.39	**0.005**	1,54	8.69	**0.005**	1,54	12.8	**<0.001**	5,270	0.002	0.97	1,54	1.22	0.30	5,270	23.9	**<0.001**	5,270	0.93	0.46	2,570
MNT																					
Base	0.05	0.82	1,54	0.01	0.94	1,54	NA	NA	NA	1.33	0.25	1,54	NA	NA	NA	NA	NA	NA	NA	NA	NA
D1	7.84	**0.007**	1,54	0.02	0.88	1,54	36.5	**<0.001**	4,216	2.03	0.16	1,54	1.17	0.32	4,216	0.47	0.76	4,216	0.83	0.51	4,216
Dark	2.75	0.10	1,54	1.41	0.24	1,54	28.1	**<0.001**	6,324	2.62	0.11	1,54	1.04	0.40	6,324	1.04	0.40	6,324	1.02	0.41	6,324
D2	4.82	**0.03**	1,54	5.73	**0.02**	1,54	197	**<0.001**	5,270	1.68	0.20	1,54	2.57	**0.03**	5,270	9.90	**<0.001**	5,270	2.82	**0.02**	5,270
DMNT																					
Base	0.60	0.44	1,54	0.91	0.34	1,54	NA	NA	NA	3.52	0.07	1,54	NA	NA	NA	NA	NA	NA	NA	NA	NA
D1	66.3	**<0.001**	1,54	2.55	0.12	1,54	81.4	**<0.001**	4,216	0.69	0.41	1,54	65.1	**<0.001**	4,216	0.62	0.65	4,216	1.10	0.36	4,216
Dark	2.34	0.13	1,54	0.45	0.50	1,54	10.7	**<0.001**	6,324	0.51	0.48	1,54	1.05	0.40	6,324	0.20	0.98	6,324	0.30	0.94	6,324
D2	7.01	**0.01**	1,54	155	**<0.001**	1,54	52.4	**<0.001**	5,270	3.67	0.06	1,54	1.74	0.13	5,270	54.6	**<0.001**	5,270	2.09	0.07	5,270
TMTT																					
Base	0.12	0.73	1,54	0	0.99	1,54	NA	NA	NA	2.23	0.14	1,54	NA	NA	NA	NA	NA	NA	NA	NA	NA
D1	8.91	**0.004**	1,54	0.67	0.42	1,54	3.05	**0.02**	4,216	0.01	0.92	1,54	1.43	0.23	4,216	0.58	0.68	4,216	0.43	0.79	4,216
Dark	2.68	0.11	1,54	0.33	0.57	1,54	7.67	**<0.001**	6,324	1.43	0.24	1,54	1.22	0.30	6,324	0.46	0.84	6,324	2.00	0.07	6,324
D2	5.83	**0.02**	1,54	15.2	**<0.001**	1,54	5.28	**<0.001**	5,270	0.01	0.93	1,54	0.35	0.88	5,270	1.69	0.14	5,270	1.03	0.40	5,270

Discussion

Herbivore-induced plant volatiles (HIPVs) play an important role in mediating interactions between damaged and undamaged plants [2]. However, the kinetics and temporal dynamics of this information transfer remain poorly understood. We show that, somewhat surprisingly, upon continuous exposure to HIPVs, receiver plants show a pronounced activation of defenses at the onset of the second day. We find that this is the result of volatile-mediated priming on the first day that yields a strong clocked response to the volatiles that are perceived on the next day. Here, we discuss the mechanisms and biological implications of this phenomenon.

Plants are well known to respond to herbivore-induced volatiles by increasing their own defenses. Defense activation can happen directly, with plants increasing their defense hormone production and volatile release [8,10], and/or via priming effects, with plants increasing their defenses more strongly upon a secondary stimulus [5,7]. Here, we show that these two phenomena operate together to trigger strong defense activation in receiver plants with predictable temporal kinetics. So far, studies in maize and other plants showing priming effects have often exposed receiver plants to HIPVs for several hours, overnight, or even for multiple days, and induced them, e.g. by simulated herbivory, on the following day in the absence of HIPVs [5,8,35–37]. Indeed, such a setup would reveal clear priming, with minor or no direct induction by the volatile treatment. Our findings demonstrate that more natural continuous exposure to volatiles results in the same pattern without the need of another stimulus. We thus conclude that HIPVs are sufficient to trigger robust, clocked defense activation in neighboring plants.

What is the mechanism that results in a strong activation of defenses on the onset of the second day of exposure to HIPVs? In maize, green leaf volatiles (GLVs) directly induce and

prime jasmonate production and terpene release [7,8,10]. Indole can prime, but not directly induce these two responses [5]. GLVs and indole again can interact to increase defense priming upon a secondary stimulus [7]. Given these considerations, together with the observed volatile release, response kinetics, and our manipulative experiments, we can draw up the following scenario: On day one, maize plants are exposed to GLVs, which trigger a small burst of terpene release in receiver plants. At the same time, receiver plants are primed to respond more strongly on the next day. At the onset of the second day, three things happen simultaneously. First, the emission of GLVs from the neighboring plants increases. Second, the defense priming mechanism responding to these cues kicks into gear. Third, terpene production and release are activated. Together, these elements result in a strong terpene burst. The orchestration of these elements is noteworthy and results in a constant and predictable response patters under variable HIPV exposure. Further experiments will reveal whether similar patterns are observed in other plants, and how they may operate on a mechanistic level. Our experiments reveal the importance of tracking plant defense responses in real time as they perceive the dynamic natural volatile blend of herbivore attacked neighbors.

What is the ecological relevance of the distinct temporal kinetics of defense activation in neighboring plants? We propose several hypotheses. First, responding most strongly to volatile cues on the second day may avoid unnecessary energy expenditure [1,13]. GLVs are emitted both upon herbivore attack and upon mechanical damage [38]. However, when damage is not sustained, GLVs will dissipate rapidly [15]. Thus, responding most strongly to repeated GLV exposure could avoid false negatives and allow plants to respond more robustly to the presence of actual herbivory. Second, sending out volatiles on the second day may maximize indirect defenses. Attracting natural enemies too early to herbivore-free plants could have fitness costs for both the plant and herbivore natural enemies. Responding on the second day could be advantageous, as by this time, the natural enemies would have located

and interacted with the herbivores on sender plants, and would thus be ready to move over to the next plant in anticipation of herbivore arrival. As fitness outcomes are likely highly nuanced, especially considering HIPVs also attract herbivores [39], investigation into information transfer on the multi-plant scale, namely in the context of multi-trophic interactions, will be critical. Considerable work will be needed to understand whether the observed defense activation pattern have any adaptive benefit.

Airborne information transfer has the potential to play a major role in plant communities, as it functions as a signaling viaduct between plants not physically connected to one another [4,7,40]. Although it has been established for decades that plants transmit airborne chemical information between individuals, we are only scratching the surface of the dynamic nature of this phenomenon. The kinetics of information transfer at the detailed temporal resolution of this study provide some insights regarding how HIPVs act across time and space. On this basis, a more comprehensive understanding of volatile-mediated information transfer between plants can be built.

Methods

Plant and insect growth

Zea mays (maize, B73) was used throughout this study. Maize plants were grown in commercial potting soil (Selmaterra, BiglerSamen, Switzerland) in 180 ml pots. Plants were grown in a greenhouse supplemented with artificial lights (300 µmol m^{-2} s^{-1}). The greenhouse was maintained at 22 ± 2 °C, 40–60% relative humidity, with a 14 h : 10 h, light : dark cycle. Two-week-old maize seedlings were used for all experiments. *Spodoptera exigua* (Frontier

Agricultural Sciences, USA) were reared from eggs on artificial diet [41] and used for experiments when they reached the 4th instar stage.

Herbivore treatment and experimental setup

The herbivore treatment consisted of adding three 4th instar larvae onto plants (sender plants). Two principal experimental setups were used to determine the kinetics of herbivore-induced plant volatile (HIPV) emissions in both sender plants (damaged by herbivores) and receiver plants (exposed to HIPVs from sender plants).

Setup 1

Single plants (senders) in transparent glass chambers (Ø×H 12 × 45 cm) were connected with PTFE tubing to a second transparent glass chamber that was either left empty or filled with a second plant (receiver). Chambers were sealed other than an airflow inlet on the first chamber and an air outlet on the second chamber, allowing HIPVs from sender plants to pass through the second chamber. Cumulative HIPV emissions from senders and receivers were measured as described in the section “Volatile emission sampling”. In order to determine emissions from receiver plants alone, HIPV emissions from sender plants connected to an empty chamber were subtracted from sender plants connected to receiver plants (Supplemental fig 1).

Setup 2

To isolate emissions solely from receiver plants, chambers containing sender and receiver plants were initially kept separate for basal HIPV emission profiling. Chambers were then

connected as in setup 1 for 30 min before herbivore treatment. After herbivores were added to sender plants, chambers remained connected for 1.25 hr, after which time sender and receiver plants were once again disconnected and rearranged so that receiver plants had both clean air flowing through the inlet and an outlet for volatile collection and profiling (Supplemental fig 1).

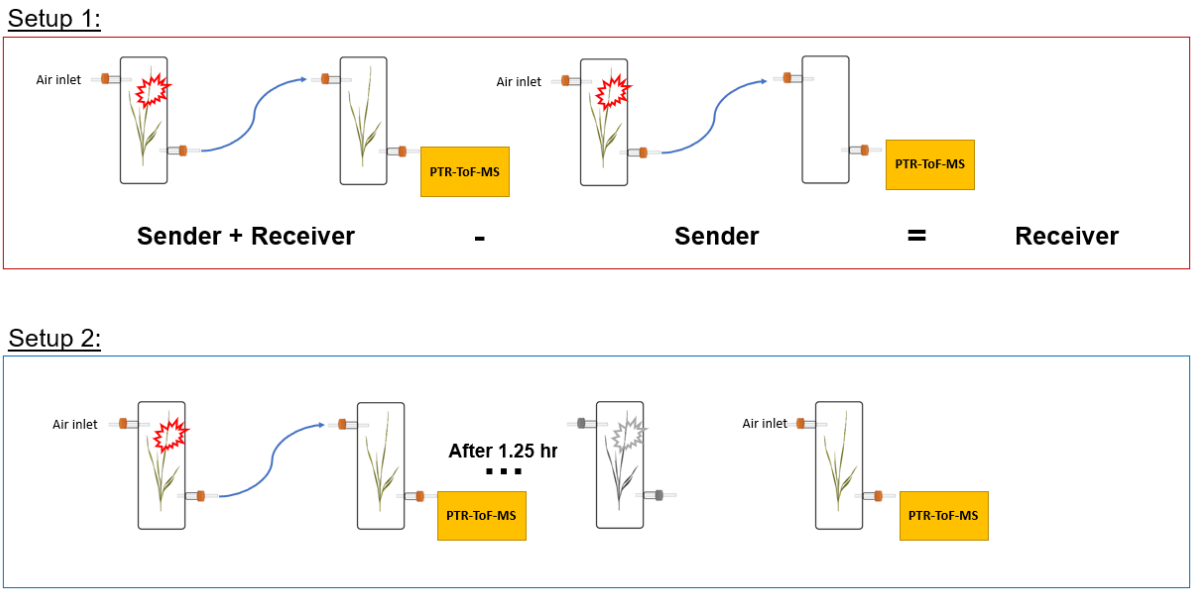

Supplemental figure 1. Experimental setup schemes for volatile profiling

Preparation of (*Z*)-3-hexenyl acetate dispensers

(*Z*)-3-hexenyl acetate dispensers were prepared as previously described with modifications [7,10]. In brief, 1.5-ml glass vials (Ø×H 11.6 × 32 mm) containing *ca.* 100 mg glass wool were filled with 200 µl (*Z*)-3-hexenyl acetate (>98%; Sigma-Aldrich, Buchs, Switzerland) diluted 50 fold in EtOH and sealed with screw caps containing a rubber septum. The caps were pierced with a 1-µl glass capillary and sealed with PTFE tape. Vials were then covered with aluminum foil and equilibrated for at least 5 days before using. Dispensers that emitted *ca.* 10x the hexenyl acetate emission from herbivore-infested plants were used. All three

GLVs measured in this study are known to be bioactive, and dispensers within the range of total GLV emission were selected [8,42].

Volatile emission sampling

Volatile emissions were collected using setup 1 and 2. Volatile profiling was measured with a high-throughput platform comprised of a proton transfer reaction time-of-flight mass spectrometer (PTR-ToF-MS; Tofwerk, Switzerland) and an automated headspace sampling system (Abon Life Sciences, Switzerland) supplied with clean airflow (0.8 L min^{-1}). An outlet on receiver plants was accessible to the autosampler/PTR-ToF-MS system. The PTR-ToF-MS system drew air at 0.1 L min^{-1}. Between samples, a zero gas measurement was performed for 3 s to avoid contamination. At each time point volatiles were continuously measured for 15-25 s and averaged to a single mean per sample. Complete mass spectra (0-500 m/z) were recorded in positive mode at *ca.* 10 Hz. The PTR was operated at 100 ˚C and an E/N of approximately 120 Td. The volatile data extraction and processing were conducted using Tofware software package v3.2.2 (Tofwerk, Switzerland). Protonated compounds were identified based on their molecular weight + 1. During volatile collection LED lights (DYNA, heliospectra) were placed *ca.* 80 cm above the glass cylinders and provided light at *ca.* 300 μmol m^{-2} s^{-1}. Identical light:dark cycle timing as the greenhouse for plant growth was used.

Foliar terpene pools and gene expression

Setup 1 was used to determine terpene pools and gene expression. After 3, 8, 16.75 and 22 hr of exposure to HIPVs, the oldest developing leaf of receiver plants was harvested and flash

frozen on liquid nitrogen. A new set of plants was used for each time point. Analysis of foliar terpene pools was conducted using slightly modified, previously described, methods [43]. In brief, *ca.* 15 mg of ground fresh frozen leaf tissue was added to a 20-ml precision thread headspace glass vial sealed with a magnetic screw cap fitted with a silicone/PTFE septum (Gertel GmbH & Co. KG, German). Immediately after a vial was prepared, an SPME fiber (100 µm polydimethylsiloxane coating; Supelco, USA) was inserted into the vial and volatiles were collected for 40 min at 50 ˚C. After collection, volatiles were thermally desorbed for 3 min at 220 ˚C and analyzed using GC-MS (Agilent, USA). He was used as the carrier gas at a flow-rate of 1 ml min^{-1} with a temperature gradient of 5 ˚C/min from 60 ˚C (1 min hold) to 250 ˚C. For quantification of gene expression, total RNA was extracted and purified from *ca*. 80 mg ground fresh frozen tissue using the GeneJET plant RNA extraction kit following the manufacturer's instructions. Genomic DNA was removed from 1 µg purified RNA using gDNA Eraser (PrimeScript RT Reagent Kit, Perfect Real Time) following manufacturer's instructions (Takara Bio Inc., Kusatsu, Japan). Reverse transcription and cDNA was synthesized using PrimeScript Reverse Transcriptase (TaKaRa Bio). Gene expression was determined with quantitative reverse transcription polymerase chain reaction (qRT-PCR) using ORA SEE qPCR Mix (highQu GmbH, Germany) on an Applied Biosystems QuantStudio 5 Real-Time PCR system. The normalized expression (NE) values were calculated as: $NE=(1/(PE_{target}^{Cttarget}))/(1/(PE_{reference}^{Ctreference}))$ where PE = primer efficiency and Ct = cycle threshold [44]. Ubiquitin (UBI1) was used as the reference gene. Gene identifiers and primer sequences are listed in Supplemental Table 1.

Supplemental Table 1. Gene identifiers and qRT-PCR primer sequences used in this study.

Target gene	Gene name	Identifier	fw	rv
TPS2	Terpene synthase 2	Zm00001d015053	TACCGGGTCGAGATCACCAA	TCGTTCGTAACGGTGTGGAG
TPS10	Terpene synthase 10	Zm00001d024486	TGACAGCCTTGATCACCGTA	AGTTCATCCCCACACGAATC
FPPS3	Farnesyl pyrophosphate synthase 3	Zm00001d043727	CCTGGCTAGTTGTGCAAGCT	CAAAACAGTTTGGACTGCCT
CYP92C5	Dimethylnonatriene/ trimethyltridecatetraene synthase	Zm00001d018839	AGGGGTTCAAGCGGAAGATG	AGGTCAGTCGCCACAAACTC
OPR7	Oxo-phytodienoate reductase 7	Zm00001d032049	GCACGCATGTGATTTGATTATTAGT	CAA TCG CGG CAT TAC CCA GAT GT
UBI1	Ubiquitin	Zm00001d015327	TAAGCTGCCGATGTGCCTGCG	CTGAAAGACAGAACATAATGAGCACAG

Phytohormone quantification

Plant treatments and tissue collection were identical for phytohormone, foliar terpene, and gene expression analysis. The phytohormones jasmonic acid (JA), JA-isoleucine (JA-Ile) and 12-oxo-phytodienoic acid (OPDA) were extracted and quantified using a slightly modified version of the method detailed in [45]. In brief, *ca.* 80 mg of finely ground fresh frozen was extracted with 1 ml ethylacetate:formic acid (99.5:0.5, v/v) spiked with isotopically labelled forms of the abovementioned phytohormones. Extracts were dried and re-suspended in 200 µl 50% MeOH using a sonicating bath for 30 min. Phytohormones were quantified using UPLC-MS-MS fitted with an Acuity BEH C18 column (Waters, USA) using a flow-rate of 400 µl/min and an injection volume of 2 µl. The two mobile phases used were 0.05% formic acid in water (A) and 0.05% formic acid in acetonitrile (B) with the following gradient conditions: 5-50% B over 5 min, 60-100% B over 3 min, 100% B for 4 min and a final re-equilibration at 5% B for 4 min.

Statistical analyses

All statistical analyses were performed in R version 4.2.2 [46]. Volatile emissions were analyzed by aligned rank transformed nonparametric factorial repeated measures ANOVA using the package ARTool, as individual plant emission kinetics were measured repeatedly over time [47]. Internal terpene pools, gene expression and phytohormone levels were analyzed using Welch's *t*-tests between control and HIPV-exposed receiver plants within each time point.

Data availability statement

All data used to generate figures and tables presented in this study are available as supplemental material (Appendix A).

Acknowledgements

The authors would like to thank Dr. Gaétan Glauser for assistance with processing samples for phytohormone quantification. We would further like to thank Dr. Bernardus Schimmel for assistance with gene expression quantification. Additionally, we thank all members of the Biotic Interactions group at the University of Bern for helpful discussions. This work was supported by the Swiss National Science Foundation (Grants Nr. 210651 and 200355), the State Secretariat for Education, Research, and Innovation SERI (Project CANWAS), the Horizon 2020 Marie Skłodowska-Curie Actions (Grant Nr. 886651) and the University of Bern.

Author Contributions

JMW and ME conceived the project. JMW, LW and ME designed specific experiments. JMW and TMC conducted experiments. JMW and ME analyzed and interpreted data. JMW wrote the initial draft of the manuscript with critical revisions from ME and input from all authors.

References

1. Waterman JM, Cazzonelli CI, Hartley SE, Johnson SN. Simulated Herbivory: The Key to Disentangling Plant Defence Responses. Trends Ecol. Evol. 2019; 34:447–58. doi: 10.1016/j.tree.2019.01.008.

2. Escobar-Bravo R, Lin P-A, Waterman JM, Erb M. Dynamic environmental interactions shaped by vegetative plant volatiles. Nat. Prod. Rep. 2023. doi: 10.1039/D2NP00061J.

3. Meents AK, Mithöfer A. Plant-Plant Communication: Is There a Role for Volatile Damage-Associated Molecular Patterns. Front. Plant Sci. 2020; 11:583275. Epub 2020/10/15. doi: 10.3389/fpls.2020.583275 PMID: 33178248.

4. Karban R. Plant Communication. Annu. Rev. Ecol. Evol. Syst. 2021; 52:1–24. doi: 10.1146/annurev-ecolsys-010421-020045.

5. Erb M, Veyrat N, Robert CAM, Xu H, Frey M, Ton J, et al. Indole is an essential herbivore-induced volatile priming signal in maize. Nat. Commun. 2015; 6:6273. Epub 2015/02/16. doi: 10.1038/ncomms7273 PMID: 25683900.

6. Kalske A, Shiojiri K, Uesugi A, Sakata Y, Morrell K, Kessler A. Insect Herbivory Selects for Volatile-Mediated Plant-Plant Communication. Curr. Biol. 2019; 29:3128-3133.e3. Epub 2019/09/12. doi: 10.1016/j.cub.2019.08.011 PMID: 31522939.

7. Hu L, Ye M, Erb M. Integration of two herbivore-induced plant volatiles results in synergistic effects on plant defence and resistance. Plant Cell Environ. 2019; 42:959–71. Epub 2018/10/16. doi: 10.1111/pce.13443 PMID: 30195252.

8. Engelberth J, Alborn HT, Schmelz EA, Tumlinson JH. Airborne signals prime plants against insect herbivore attack. Proc. Natl. Acad. Sci. U.S.A. 2004; 101:1781–5. doi: 10.1073/pnas.0308037100.

9. Vázquez-González C, Quiroga V, Martín-Cacheda L, Rasmann S, Röder G, Abdala-Roberts L, et al. Effect of herbivore load on VOC-mediated plant communication in potato. Planta. 2023; 257:42. doi: 10.1007/s00425-023-04075-6.

10. Wang L, Jäggi S, Walthert M, Waterman JM, Cofer TM, Erb M. Immature leaves are the dominant volatile (Z)-3-hexenyl acetate sensing organs of maize. bioRxiv. 2023:2023.01.12.523648. doi: 10.1101/2023.01.12.523648.

424 **11**. Ruther J, Fürstenau B. Emission of herbivore-induced volatiles in absence of a herbivore--
425 response of Zea mays to green leaf volatiles and terpenoids. Z. Naturforsch. C. 2005; 60:743–
426 56. doi: 10.1515/znc-2005-9-1014 PMID: 16320618.
427 **12**. Mauch-Mani B, Baccelli I, Luna E, Flors V. Defense Priming: An Adaptive Part of Induced
428 Resistance. Annu. Rev. Plant Biol. 2017; 68:485–512. doi: 10.1146/annurev-arplant-042916-
429 041132.
430 **13**. Mithöfer A, Wanner G, Boland W. Effects of feeding Spodoptera littoralis on lima bean leaves.
431 II. Continuous mechanical wounding resembling insect feeding is sufficient to elicit herbivory-
432 related volatile emission. Plant Physiol. 2005; 137:1160–8. doi: 10.1104/pp.104.054460 PMID:
433 15728342.
434 **14**. Yu X, Feng B, He P, Shan L. From Chaos to Harmony: Responses and Signaling upon Microbial
435 Pattern Recognition. Annu. Rev. Phytopathol. 2017; 55:109–37. doi: 10.1146/annurev-phyto-
436 080516-035649.
437 **15**. D'Auria JC, Pichersky E, Schaub A, Hansel A, Gershenzon J. Characterization of a BAHD
438 acyltransferase responsible for producing the green leaf volatile (Z)-3-hexen-1-yl acetate in
439 Arabidopsis thaliana. Plant J. 2007; 49:194–207. Epub 2006/12/06. doi: 10.1111/j.1365-
440 313X.2006.02946.x PMID: 17163881.
441 **16**. Matsui K. Green leaf volatiles: hydroperoxide lyase pathway of oxylipin metabolism. Curr.
442 Opin. Plant. Biol. 2006; 9:274–80. doi: 10.1016/j.pbi.2006.03.002.
443 **17**. Ye M, Liu M, Erb M, Glauser G, Zhang J, Li X, et al. Indole primes defence signalling and
444 increases herbivore resistance in tea plants. Plant. Cell. Environ. 2021; 44:1165–77. Epub
445 2020/11/02. doi: 10.1111/pce.13897 PMID: 32996129.
446 **18**. Ye M, Veyrat N, Xu H, Hu L, Turlings TCJ, Erb M. An herbivore-induced plant volatile reduces
447 parasitoid attraction by changing the smell of caterpillars. Sci. Adv. 2018; 4:eaar4767. Epub
448 2018/05/16. doi: 10.1126/sciadv.aar4767 PMID: 29774237.
449 **19**. Veyrat N, Robert CAM, Turlings TCJ, Erb M. Herbivore intoxication as a potential primary
450 function of an inducible volatile plant signal. J Ecol. 2016; 104:591–600. doi: 10.1111/1365-
451 2745.12526.
452 **20**. Chen C, Chen H, Huang S, Jiang T, Wang C, Tao Z, et al. Volatile DMNT directly protects plants
453 against Plutella xylostella by disrupting the peritrophic matrix barrier in insect midgut. Elife.
454 2021; 10. Epub 2021/02/18. doi: 10.7554/eLife.63938 PMID: 33599614.
455 **21**. Zhou F, Pichersky E. More is better: the diversity of terpene metabolism in plants. Curr Opin
456 Plant Biol. 2020; 55:1–10. Epub 2020/02/20. doi: 10.1016/j.pbi.2020.01.005 PMID: 32088555.
457 **22**. Riedlmeier M, Ghirardo A, Wenig M, Knappe C, Koch K, Georgii E, et al. Monoterpenes Support
458 Systemic Acquired Resistance within and between Plants. Plant Cell. 2017; 29:1440–59.
459 doi: 10.1105/tpc.16.00898 PMID: 28536145.
460 **23**. Seidl-Adams I, Richter A, Boomer KB, Yoshinaga N, Degenhardt J, Tumlinson JH. Emission of
461 herbivore elicitor-induced sesquiterpenes is regulated by stomatal aperture in maize (*Zea*
462 *mays*) seedlings. Plant Cell Environ. 2015; 38:23–34. doi: 10.1111/pce.12347.
463 **24**. He J, Halitschke R, Schuman MC, Baldwin IT. Light dominates the diurnal emissions of
464 herbivore-induced volatiles in wild tobacco. BMC Plant Biol. 2021; 21:401.
465 doi: 10.1186/s12870-021-03179-z.
466 **25**. Bläsing OE, Gibon Y, Günther M, Höhne M, Morcuende R, Osuna D, et al. Sugars and circadian
467 regulation make major contributions to the global regulation of diurnal gene expression in
468 Arabidopsis. Plant Cell. 2005; 17:3257–81. doi: 10.1105/tpc.105.035261 PMID: 16299223.
469 **26**. Lin P-A, Chen Y, Ponce G, Acevedo FE, Lynch JP, Anderson CT, et al. Stomata-mediated
470 interactions between plants, herbivores, and the environment. Trends Plant Sci. 2022; 27:287–
471 300. doi: 10.1016/j.tplants.2021.08.017.

472 **27**. Caird MA, Richards JH, Donovan LA. Nighttime Stomatal Conductance and Transpiration in C3
473 and C4 Plants. Plant Physiol. 2007; 143:4–10. doi: 10.1104/pp.106.092940.
474 **28**. Loughrin JH, Manukian A, Heath RR, Turlings TC, Tumlinson JH. Diurnal cycle of emission of
475 induced volatile terpenoids by herbivore-injured cotton plant. Proc. Natl. Acad. Sci. U.S.A.
476 1994; 91:11836–40. doi: 10.1073/pnas.91.25.11836 PMID: 11607499.
477 **29**. Block AK, Vaughan MM, Schmelz EA, Christensen SA. Biosynthesis and function of terpenoid
478 defense compounds in maize (Zea mays). Planta. 2019; 249:21–30. doi: 10.1007/s00425-018-
479 2999-2.
480 **30**. Richter A, Seidl-Adams I, Köllner TG, Schaff C, Tumlinson JH, Degenhardt J. A small,
481 differentially regulated family of farnesyl diphosphate synthases in maize (Zea mays) provides
482 farnesyl diphosphate for the biosynthesis of herbivore-induced sesquiterpenes. Planta. 2015;
483 241:1351–61. doi: 10.1007/s00425-015-2254-z PMID: 25680349.
484 **31**. Richter A, Schaff C, Zhang Z, Lipka AE, Tian F, Köllner TG, et al. Characterization of Biosynthetic
485 Pathways for the Production of the Volatile Homoterpenes DMNT and TMTT in Zea mays. Plant
486 Cell. 2016; 28:2651–65. Epub 2016/09/23. doi: 10.1105/tpc.15.00919 PMID: 27662898.
487 **32**. Martin DM, Gershenzon J, Bohlmann J. Induction of Volatile Terpene Biosynthesis and Diurnal
488 Emission by Methyl Jasmonate in Foliage of Norway Spruce. Plant Physiol. 2003; 132:1586–99.
489 doi: 10.1104/pp.103.021196.
490 **33**. Ament K, Kant MR, Sabelis MW, Haring MA, Schuurink RC. Jasmonic acid is a key regulator of
491 spider mite-induced volatile terpenoid and methyl salicylate emission in tomato. Plant Physiol.
492 2004; 135:2025–37. doi: 10.1104/pp.104.048694 PMID: 15310835.
493 **34**. Yan Y, Christensen S, Isakeit T, Engelberth J, Meeley R, Hayward A, et al. Disruption of OPR7
494 and OPR8 Reveals the Versatile Functions of Jasmonic Acid in Maize Development and
495 Defense. Plant Cell. 2012; 24:1420–36. doi: 10.1105/tpc.111.094151.
496 **35**. Ton J, D'Alessandro M, Jourdie V, Jakab G, Karlen D, Held M, et al. Priming by airborne signals
497 boosts direct and indirect resistance in maize. Plant J. 2007; 49:16–26. doi: 10.1111/j.1365-
498 313X.2006.02935.x.
499 **36**. Ali M, Sugimoto K, Ramadan A, Arimura G. Memory of plant communications for priming anti-
500 herbivore responses. Sci. Rep. 2013; 3:1872. doi: 10.1038/srep01872.
501 **37**. Paudel Timilsena B, Seidl-Adams I, Tumlinson JH. Herbivore-specific plant volatiles prime
502 neighboring plants for nonspecific defense responses. Plant Cell Environ. 2020; 43:787–800.
503 doi: 10.1111/pce.13688 PMID: 31759336.
504 **38**. Gardiner B, Berry P, Moulia B. Review: Wind impacts on plant growth, mechanics and damage.
505 Plant Sci. 2016; 245:94–118. doi: 10.1016/j.plantsci.2016.01.006.
506 **39**. Zu P, Boege K, Del-Val E, Schuman MC, Stevenson PC, Zaldivar-Riverón A, et al. Information
507 arms race explains plant-herbivore chemical communication in ecological communities.
508 Science. 2020; 368:1377–81. doi: 10.1126/science.aba2965.
509 **40**. Wenig M, Ghirardo A, Sales JH, Pabst ES, Breitenbach HH, Antritter F, et al. Systemic acquired
510 resistance networks amplify airborne defense cues. Nat. Commun. 2019; 10:3813. Epub
511 2019/08/23. doi: 10.1038/s41467-019-11798-2 PMID: 31444353.
512 **41**. Maag D, Dalvit C, Thevenet D, Köhler A, Wouters FC, Vassão DG, et al. 3-β-D-Glucopyranosyl-6-
513 methoxy-2-benzoxazolinone (MBOA-N-Glc) is an insect detoxification product of maize 1,4-
514 benzoxazin-3-ones. Phytochem. 2014; 102:97–105. doi: 10.1016/j.phytochem.2014.03.018
515 PMID: 24713572.
516 **42**. Matsui K, Sugimoto K, Mano J, Ozawa R, Takabayashi J. Differential metabolisms of green leaf
517 volatiles in injured and intact parts of a wounded leaf meet distinct ecophysiological
518 requirements. PLOS ONE. 2012; 7:e36433. doi: 10.1371/journal.pone.0036433 PMID:
519 22558466.

520 **43**. Escobar-Bravo R, Schimmel BCJ, Glauser G, Klinkhamer PGL, Erb M. Leafminer attack
521 accelerates the development of soil-dwelling conspecific pupae via plant-mediated changes in
522 belowground volatiles. New Phytol. 2022; 234:280–94. doi: 10.1111/nph.17966.
523 **44**. Alba JM, Schimmel BCJ, Glas JJ, Ataide LMS, Pappas ML, Villarroel CA, et al. Spider mites
524 suppress tomato defenses downstream of jasmonate and salicylate independently of hormonal
525 crosstalk. New Phytol. 2015; 205:828–40. doi: 10.1111/nph.13075.
526 **45**. Glauser G, Vallat A, Balmer D. Hormone profiling. Methods Mol Biol. 2014; 1062:597–608.
527 doi: 10.1007/978-1-62703-580-4_31 PMID: 24057388.
528 **46**. R Core Team. R: A language and environment for statistical computing. Vienna, Austria: R
529 Foundation for Statistical Computing; 2022.
530 **47**. Wobbrock JO, Findlater L, Gergle D, Higgins JJ. The aligned rank transform for nonparametric
531 factorial analyses using only anova procedures. Proceedings of the SIGCHI Conference on
532 Human Factors in Computing Systems. Vancouver, BC, Canada: Association for Computing
533 Machinery; 2011. pp. 143–6.